Pergamon

PII: S0043-1354(98)00194-8

Wat. Res. Vol. 33, No. 1, pp. 43–52, 1999

Printed in Great Britain
0043-1354/98 $ - see front matter

PHYSICOCHEMICAL MECHANISMS RESPONSIBLE FOR THE FILTRATION AND MOBILIZATION OF A FILAMENTOUS BACTERIOPHAGE IN QUARTZ SAND

JEREMY A. REDMAN[1], STANLEY B. GRANT[1]*, TERESE M. OLSON[1], JESSICA M. ADKINS[1], JAMES L. JACKSON[2], MILAGROS S. CASTILLO[2] and WILLIAM A. YANKO[2]Ⓜ

[1]Department of Civil and Environmental Engineering, University of California, Irvine, CA 92697, U.S.A. and [2]San Jose Creek Water Quality Laboratory, County Sanitation Districts of Los Angeles County, Whittier, CA 90601, U.S.A.

(First received September 1997; accepted in revised form April 1998)

Abstract—This study examines the influence of pore water chemistry on the filtration and physicochemical properties of a male-specific filamentous bacteriophage isolated from chlorinated effluent of the San Jose Creek Water Reclamation Plant in Los Angeles County, California. The isolate belongs to a class of bacteriophage that are naturally present in sources of sewage, and hence may be an indicator of fecal contamination in groundwater. Furthermore, there is some evidence that this class of bacteriophage are mobilized in the subsurface following rainfall events, although the mechanism responsible for this process is not yet clear. Using a model filtration system consisting of packed columns of quartz sand, we found that the filtration of this isolate was strongly dependent on the concentration and valence of the dominant cation in the pore fluid. In one set of experiments involving columns 19 cm in length, virus retention in the column increased from 0% to 99.999% when the electrolyte composition of the pore fluid was changed from 10 mM NaCl to 10 mM $CaCl_2$. With one exception, filtration efficiencies calculated from the column experiments were inversely proportional to the electrophoretic mobility of the virus, implying that electrostatic interactions between the virus and the quartz surface dominate the filtration dynamics of this particular bacteriophage. From a practical perspective, these results indicate that small changes in the hardness and total dissolved solids of pore fluids –as might occur following a rainfall event– can dramatically affect both the filtration and mobilization of filamentous bacteriophage in subsurface systems.

Key words—filamentous bacteriophage, virus, filtration, electrophoretic mobility, electrostatics

INTRODUCTION

Groundwater can serve as a vector for the transmission of Norwalk virus and other human enteric viruses (Keswick and Gerba, 1980; Lawson *et al.*, 1991; Hedberg and Osterholm, 1993), although the environmental factors that promote the subsurface transport of waterborne viral pathogens are largely unknown. We have conducted several studies to assess the geochemical features of subsurface systems that influence the physicochemical filtration of viruses as they move from sources of human waste (such as septic tank fields, groundwater recharge basins, broken sewer lines, etc.) toward groundwater wells used for irrigation and/or municipal supply (Grant *et al.*, 1993; Penrod *et al.*, 1996; Redman *et al.*, 1997). Many of the waterborne viruses of most direct concern to human health cannot be easily cultivated in the laboratory, and consequently bacteriophage are routinely used as surrogates for enteric viruses in both laboratory and field investigations (Reddy *et al.*, 1981; Snowdon and Cliver, 1989; IAWPRC, 1991). The male-specific coliphage appear to be particularly promising in this regard, because (i) their coliform host is present in high concentrations in the feces of humans and other warm blooded animals, and hence these bacteriophage are likely to be good indicators of fecal contamination, and (ii) their receptor on the host cell (the male pilus) is only expressed at temperatures above 25–30°C (Havelaar and Pot-Hogeboom, 1988; Woody and Cliver, 1995), and therefore they are unlikely to replicate in groundwater systems. Of the male-specific coliphage, the icosahedral RNA bacteriophage like MS2 are most commonly used for filtration studies, primarily because they are morphologically similar to the human enteric viruses (Havelaar *et al.*, 1993).

In this study, we investigated the physicochemical mechanisms responsible for the filtration and mobilization of a male-specific coliphage isolated from the effluent of a wastewater reclamation plant in Southern California. The isolate (referred to as

*Author to whom all correspondence should be addressed. [Tel.: +1-949-824-7320; Fax: +1-949-824-3672; E-mail: sbgrant@uci.edu].

SJC3) is a single-stranded DNA (ssDNA) filamentous bacteriophage. Based on electron micrographs of the virus and previous characterization of its genome (Yanko *et al.*, 1998), SJC3 is a F1-type member of the Inoviridae family of bacteriophage (Ackermann, 1996). There are several reasons why this particular subclass of male-specific bacteriophage are interesting from the perspective of groundwater contamination, despite the fact that they bear no morphological similarity to the human enteric viruses. As documented in a companion paper (Yanko *et al.*, 1998), these bacteriophage survive conventional wastewater treatment processes – including primary settling, secondary aeration, filtration through dual media filters, chlorination, and de-chlorination– and have been detected in surface water and groundwater. The spatio-temporal pattern of the groundwater isolates suggested these phage may be mobilized in the subsurface following rainfall events. Hence, their presence or absence in groundwater may be a sensitive indicator of water purity. In addition, a filamentous bacteriophage of *Vibrio cholera* has recently been implicated in the lysogenic conversion of this bacteria to the toxic form, suggesting that at least some filamentous bacteriophage are indirectly involved in waterborne disease transmission (Waldor and Mekalanos, 1996). For the set of experiments described here, we investigated the electrostatic properties of SJC3 and its filtration in packed beds of ultra-clean quartz sand. We find that the filtration of the virus is extremely sensitive to the electrolyte composition of the pore fluid, with more filtration generally occurring as the ionic strength and the hardness of the water increases. These results are interpreted in the context of colloid filtration theory, and the role electrostatic repulsive forces play in the deposition kinetics of the virus.

MATERIALS AND METHODS

Bacteriophage purification

The filamentous male-specific coliphage used in this study, designated SJC3, was obtained from W. Yanko as a plaque purified culture originally isolated from tertiary filtered, chlorinated final effluent from the San Jose Creek Water Reclamation Plant following procedures previously documented (Yanko *et al.*, 1998). The bacteriophage was purified following the method presented by Dai *et al.* (1990). Briefly, plate lysates were pooled and centrifuged for 10 min at $6000 \times g$ in a Sorvall RC 28S (Du Pont Company, Wilmington, DE) at 4°C. The supernatant was collected and polyethylene glycol (m.w. 8000) and NaCl were added to final concentrations of 3% and 0.5% respectively. The mixture was stirred for 1 h and the bacteriophage was allowed to precipitate at 4°C overnight. Following centrifugation at $6000 \times g$ for 10 min at 4°C, the supernatant was poured off and the precipitate was resuspended in approximately 8 ml of tryptone broth (Difco, Detroit, MI). The concentrated virus solution was layered onto a CsCl step gradient with layers of the following densities: 1.18, 1.25, 1.34, and 1.39 g/ml. The gradient was centrifuged at 23,000 rpm for 24 h at 4°C in an Optima LE-80K Ultracentrifuge using an SW 41 Ti rotor (Beckman Instruments, Fullerton, CA). The band of purified virus was collected by side puncture and aliquots of the purified bacteriophage stock were dialyzed repeatedly against 3 l of a 10 mM electrolyte solution (either NaCl, $CaCl_2$, or $MgCl_2$) using Slide-A-Lyzer dialysis cassettes (10,000 MWCO, Pierce, Rockford, IL).

Bacteriophage growth and enumeration

Concentrations of infective viruses were determined by the plaque-forming unit (PFU) assay using the agar overlay method (Adams, 1959; Bales *et al.*, 1991). Briefly, dilutions of each sample were mixed with host cell, *E. coli* HS(pFamp)R, plated on tryptone agar containing ampicillin and streptomycin and incubated overnight (Yanko *et al.*, 1998). The resulting plaque counts were converted to PFU/ml.

Electron microscopy sample preparation

Transmission electron microscopy measurements of SJC3 were made using a two-step negative staining technique. A 40 mesh Formvar/carbon support film grid (Electron Microscopy Science, Ft. Washington, PA) was floated, carbon side down, on top of a drop of the purified bacteriophage suspension for 20 min. Excess fluid was removed by touching the edge of the grid to a Kimwipe. The grid was then floated on a drop of 2% uranyl acetate solution for 15–20 min. The excess fluid was again removed with a Kimwipe, after which the grid was allowed to air dry. The stained viruses were visualized using a Zeiss 10CR transmission electron microscope with a beam strength of 80 kV.

Capillary microelectrophoresis

Electrolyte solutions for capillary microelectrophoresis measurements were prepared from deionized water (Milli-Q, 18.2 MΩ cm, Millipore, Bedford, MA.) and either analytical grade NaCl, $CaCl_2$, or $MgCl_2$. Solution pH was adjusted with analytical grade HCl and NaOH. Seventy μl of the bacteriophage suspension, previously dialyzed into 10 mM of the respective electrolyte solution, was diluted into 7 ml of the electrolyte solution for a final virus concentration of approximately 10^9 PFU/ml. Measurements were conducted using a Rank Brothers Mark II apparatus (Cambridge, U.K.) equipped with a 0.5 mW green (544 nm) He–Ne laser (Melles Griot Model 05 SGR 851, Melles Griot, Carlsbad, CA) and a capillary cell in a four electrode operation. It was previously determined in our laboratory that by utilizing a green laser, virus particles as small as 27 nm could be visualized in a conventional capillary cell (Penrod *et al.*, 1995). The capillary cell was flushed three times with deionized water and four times with virus-free electrolyte solution. The capillary was then filled with the electrolyte solution containing the bacteriophage and mobility measurements were carried out at temperatures between 7 and 9°C. The reported values of electrophoretic mobility generally represent the average of 40 measurements, 20 at both the upper and lower stationary levels. Exceptions include 50 measurements of particle velocity in the presence of 10 mM NaCl at pH 4.74, and 36 measurements of particle velocity in the presence of 1 mM $CaCl_2$.

Filtration experiments

The quartz sand used in the column filtration experiments was purchased from Unimin (New Canaan, CT), size-fractionated by a wet sedimentation/flotation technique, and then cleaned to remove metal and organic contaminants (Litton and Olson, 1993). The average grain diameter was determined by sieve analysis using the method of moments by weight (Folk, 1980). The cleaning steps included soaking the sand in 12 N HCl for at least

24 h, washing with deionized water (Milli-Q), and baking the sand overnight at 800°C. Cleaned sand was stored under a vacuum. Before conducting column experiments, the sand was rehydrated by boiling for at least 1 h in filtered deionized water. The filtration experiments were carried out in adjustable bed-height glass columns (Pharmacia LKB C16, Piscataway, NJ) packed by allowing the quartz sand to settle in filtered deionized water. The average porosity of the packed beds was estimated by allowing quartz sand to settle in graduated cylinders and measuring the difference in weight of the packed bed before and after the pore water was evaporated by heating at 100°C for several days. Electrolyte solutions were prepared from analytical grade NaCl, $CaCl_2$, or $MgCl_2$, and adjusted to pH 7 with NaOH and HCl. pH adjustment of electrolyte solutions resulted in a maximum increase in ionic strength of approximately 0.0003 M. The packed columns were equilibrated by pumping (Pharmacia LKB P1 peristaltic pump) approximately 10 pore volumes of the electrolyte solution of interest through the column prior to each filtration experiment. A "blank" sample was collected from the column effluent at this point and analyzed in triplicate for the presence of bacteriophage as previously described. Influent solutions were prepared by adding 25 μl of the purified bacteriophage solution to approximately 250 ml of the filtered electrolyte solution. Three separate samples were collected from the influent solution and analyzed in triplicate to determine the concentration of bacteriophage applied to the column. Column effluent was collected in 3 min increments using an automatic fraction collector (Pharmacia LKB FRAC-200). Each fraction was analyzed in triplicate for bacteriophage as previously described. For electrolyte conditions where measurable virus filtration occurred, control experiments were carried out to measure bacteriophage adsorption to the column walls. The control experiments were conducted by passing virus suspensions through the column apparatus to which no quartz sand had been added. The filtration and control experiments were conducted at 4°C.

Conductivity measurements

Five ml of the column effluent sample was added to 200 ml of Milli-Q water, and the conductivity of the resulting solution was measured (Orion model 160 conductivity meter, Boston, MA) at a temperature between 22.7 and 23.2°C.

Filtration rate constants

Filtration rate constants were calculated from the non-dispersive portion of the virus breakthrough curves using two different mathematical models of virus filtration: the deep-bed filtration model (Yao *et al.*, 1971) and the linear chromatography model (Rajagopalan and Chu, 1982). In the deep-bed filtration model, the concentration of the virus exiting the column, C, is assumed to decline exponentially with column length, L:

$$C = C_0 \exp\left(\frac{-3(1-\varepsilon)k_f L}{Ua}\right). \quad (1)$$

In this equation, C_0, ε, a, U, k_f represent, respectively, the concentration of infective virus particles in the column influent (measured in PFU/ml), bed porosity, radius of sand in the column, superficial velocity of the pore fluid, and the forward filtration rate constant. For each experiment where measurable virus filtration occurred, an estimate for the forward filtration rate constant was obtained by solving equation 1 for k_f, and substituting into the equation our estimates for the physical constants ε, L, a and U (see Table 1) and the average fractional concentration of viruses in the non-dispersive portion of the virus breakthrough curve, C/C_0. The deep-bed filtration model assumes that the effluent concentration of viruses has achieved a steady-state value, that virus filtration occurs irreversibly, and that virus deposition onto bed media is not retarded by previously deposited viruses (i.e., blocking effects are negligible, Johnson and Elimelech, 1995).

The linear chromatography model is a more sophisticated model of virus filtration which allows for the reversible deposition of viruses onto the filter media:

$$C = C_0 J\left(\frac{3k_f(1-\varepsilon)L}{Ua}, \frac{k_r L(\tau-1)\varepsilon}{U}\right). \quad (2)$$

In this equation, the reverse rate constant k_r accounts for virus detachment and τ represents the number of pore volumes that have passed through the column. The function J is defined as follows,

$$J(a,b) = 1 - e^{-b}\int_0^a e^{-x} I_0(2\sqrt{bx})\, dx, \quad (3)$$

where I_0 represents the zero-order Bessel function. Values of k_f and k_r were determined by fitting equation 2 to the virus breakthrough data using a Levenberg–Marquardt non-linear least-squares approach (Press *et al.*, 1986).

Filtration efficiency and dimensionless deposition rate

The magnitude of the forward filtration rate constant k_f is controlled by the microscale transport processes that bring a virus into close proximity to a grain in the column (referred to here as a "collector"), and the hydrodynamic and physicochemical forces that develop between the virus and collector on close approach. These two factors can be

Table 1. Physical properties of packed bed columns used in filtration and control experiments[a]

Pore fluid	Solution pH	Column length (cm)	Superficial velocity (cm/s)	Influent concentration (PFU/mL)
		Filtration experiments		
1 mM NaCl	6.9	16.8	0.025	$1.6 \pm 0.1 \times 10^7$
5 mM NaCl	6.9	34.1	0.025	$1.2 \pm 0.0 \times 10^8$
10 mM NaCl	6.9	29.8	0.025	$3.1 \pm 0.3 \times 10^7$
100 mM NaCl	6.9	19.1	0.025	$1.4 \pm 0.1 \times 10^8$
1 mM $CaCl_2$	7.0	18.7	0.025	$8.6 \pm 0.6 \times 10^6$
10 mM $CaCl_2$	7.1	19.3	0.022	$2.1 \pm 0.2 \times 10^7$
100 mM $CaCl_2$	7.0	18.7	0.022	$1.7 \pm 0.0 \times 10^7$
1 mM $MgCl_2$	6.9	16.5	0.025	$2.0 \pm 0.0 \times 10^7$
10 mM $MgCl_2$	7.1	19.1	0.025	$1.8 \pm 0.2 \times 10^7$
100 mM $MgCl_2$	7.0	15.7	0.025	$1.9 \pm 0.0 \times 10^7$
		Control experiments		
1 mM NaCl	6.9	17.0	0.025	$3.0 \pm 0.1 \times 10^8$
1 mM $MgCl_2$	7.0	19.0	0.025	$2.2 \pm 0.2 \times 10^7$
100 mM $CaCl_2$	7.0	18.9	0.023	$2.4 \pm 0.4 \times 10^7$

[a]The packed bed porosity was estimated to be $\varepsilon = 0.49 \pm 0.02$ ($n = 4$). The average grain radius was calculated to be $a = 111 \pm 16$ μm. The experimental parameters for the elution experiment were identical to those used for the 1 mM $CaCl_2$ experiment.

quantified by expressing the filtration rate constant as a product of a dimensionless deposition rate η_0 and a filtration efficiency α:

$$k_f = U\eta_0\alpha/4. \quad (4)$$

The parameter α represents the number of virus/collector collisions that result in a "sticking event", and is strongly influenced by solution chemistry. The dimensionless deposition rate η_0 represents the fraction of viruses approaching the collector that collide with the surface. Theoretical expressions for η_0 have been derived under conditions where Brownian diffusion, interception, and/or gravitational sedimentation dominate the transport of particles in the immediate vicinity of a collector (Yao *et al.*, 1971), although these expressions are valid only for spherical colloids and therefore cannot be applied to our particular system. Instead, we estimated η_0 experimentally by using a rearranged version of equation 4:

$$\eta_0^{max} = 4k_f^{100\ mM\ MgCl_2}/U, \quad (5)$$

where we have assumed that the filtration efficiency is unity (i.e., each virus/collector collision results in a sticking event), and we have used the filtration rate constant k_f corresponding to the experiment where 100 mM $MgCl_2$ was used as the pore fluid. This particular electrolyte condition was chosen because it yielded the largest value for the dimensionless deposition rate. The filtration efficiency for each filtration experiment was determined from this maximum experimental dimensionless deposition rate and k_f as follows:

$$\alpha = 4k_f/U\eta_0^{max}. \quad (6)$$

In several of the filtration experiments there was no measurable filtration; i.e. $C/C_0 \approx 1$. For these cases, a forward filtration rate constant and filtration efficiency could not be estimated directly from the breakthrough data. Instead, we estimated an "upper-limit" for the filtration rate constant k_f by assuming a breakthrough concentration C/C_0 of 0.95 in equation 1. This upper-limit for k_f was then used, in turn, to estimate an upper-limit for α from equation 6.

RESULTS

Electron microscopy analysis

TEM images of SJC3 at 50,000× magnification were used to determine the length of the virus. A single well-defined virus was measured and determined to be approximately 900 nm in length and 8 nm in diameter. These dimensions are in the range reported for other male-specific filamentous bacteriophage (Model and Russel, 1988).

Packed bed filtration

The goal of this study was to elucidate the fundamental mechanisms that control virus filtration. In order to maximize our chances of achieving this goal, we chose to work with a model system that was as reproducible and well-characterized as possible; namely, clean quartz sand as the filter media and well purified virus suspensions. Filtration experiments were conducted by suspending the purified bacteriophage isolate into an electrolyte solution, and then applying the bacteriophage suspension in a continuous fashion to the influent of a saturated column packed with well-cleaned quartz sand. The concentration of virus in the column effluent was monitored over time, and the resulting "breakthrough" data were normalized by the influent concentration of virus and plotted against the number of pore volumes passed through the column (see Fig. 1). Separate filtration experiments were conducted with three different salts (NaCl, $CaCl_2$, and $MgCl_2$) at three different electrolyte concentrations (1, 10, 100 mM); an additional filtration experiment was conducted with 5 mM NaCl. The physical properties of the packed bed columns used in each experiment are summarized in Table 1.

Each of the breakthrough curves (BTCs) plotted in Fig. 1 exhibits a characteristic pattern in which the normalized plaque-forming unit (PFU) concentration in the column effluent rises sharply between 1 and 2 pore volumes, and thereafter stabilizes at a constant value or increases slowly. In this paper we refer to the portion of the BTC after approximately 2 pore volumes as the "non-dispersive" region. For most of the filtration experiments we conducted, the non-dispersive portion of the BTCs attained a steady-state value as predicted by deep-bed filtration theory (see Materials and Methods). However, in several cases –most notably 10 mM $MgCl_2$ and 100 mM NaCl– the non-dispersive portion of the BTCs exhibit a positive slope, indicating that the filter performance diminishes over time due to either virus desorption from the column or blocking effects (Johnson and Elimelech, 1995). Importantly, the nature of the electrolyte solution dramatically influences the level of filtration achieved in the non-dispersive portion of the BTCs.

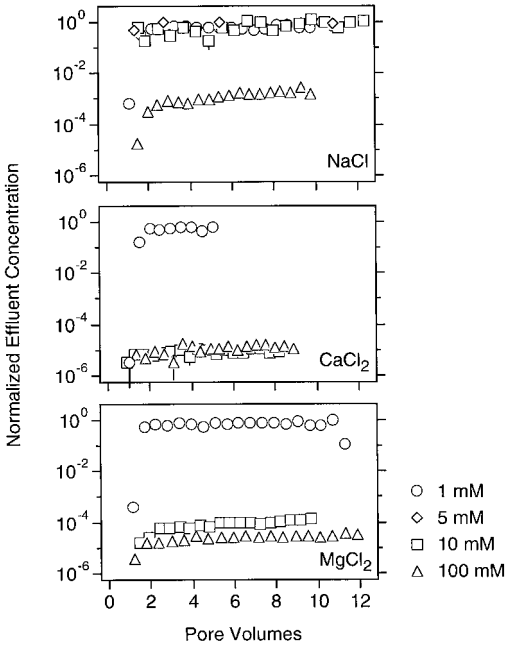

Fig. 1. Experimental virus breakthrough curves at pH 7 and the electrolyte composition noted in the figure. Influent and effluent samples were analyzed in triplicate. Error bars represent one standard deviation.

Table 2. Calculated values of forward and reverse filtration rate constants and filtration efficiencies

Pore fluid	Deep-bed model	Linear chromatography model		
	k_f (cm/s)	k_f (cm/s)	k_r (1/s)	α
1 mM NaCl	$4.8 \pm 1.9 \times 10^{-6}$	5.6×10^{-6}	8.2×10^{-5}	0.04 ± 0.01
5 mM NaCl	N.D.	N.D.	N.D.	2.2×10^{-3}[a]
10 mM NaCl	N.D.	N.D.	N.D.	2.6×10^{-3}[a]
100 mM NaCl	$6.3 \pm 1.0 \times 10^{-5}$	7.5×10^{-5}	1.4×10^{-4}	0.52 ± 0.08
1 mM $CaCl_2$	$6.1 \pm 1.1 \times 10^{-6}$	6.4×10^{-6}	9.8×10^{-5}	0.05 ± 0.01
10 mM $CaCl_2$	$9.8 \pm 1.4 \times 10^{-5}$	9.8×10^{-5}	4.6×10^{-7}	0.90 ± 0.13
100 mM $CaCl_2$	$9.8 \pm 1.5 \times 10^{-5}$	1.0×10^{-4}	2.4×10^{-5}	0.90 ± 0.13
1 mM $MgCl_2$	$4.1 \pm 3.0 \times 10^{-6}$	5.4×10^{-6}	1.5×10^{-4}	0.03 ± 0.03
10 mM $MgCl_2$	$8.7 \pm 1.3 \times 10^{-5}$	9.3×10^{-5}	4.2×10^{-5}	0.73 ± 0.11
100 mM $MgCl_2$	$1.2 \pm 0.2 \times 10^{-4}$	1.3×10^{-4}	2.0×10^{-5}	1.00 ± 0.15

[a]Upper-limit estimate obtained by assuming a breakthrough concentration of $C/C_0 = 0.95$.

In particular, we found that the normalized concentration of virus in the non-dispersive portion of the BTCs decreased as the concentration of salt in the pore fluid was increased. For example, increasing the concentration of NaCl from 10 to 100 mM resulted in a 99.9% increase in the fraction of virus retained in the column. The nature of the dominant cation also dramatically affected filter performance. When the electrolyte composition of the pore fluid was changed from 10 mM NaCl to 10 mM $CaCl_2$, for example, virus retention in the column increased from 0% to 99.999%.

As outlined in Materials and Methods, the deep-bed filtration model (DBFM, equation 1) and the linear chromatography model (LCM, equation 2) were used to calculate filtration rate constants from the non-dispersive portion of the BTCs. The resulting values of the forward filtration rate constant k_f (calculated from both the DBFM and LCM), and the reverse rate constant k_r (calculated from the LCM), are summarized for each experiment in Table 2. Differences in the forward rate constants calculated using the two models were generally small ($< 30\%$), and consequently values of k_f determined by the DBFM were used below to calculate filtration efficiencies. By choosing values of k_f calculated from the DBFM, the standard error associated with this parameter could be estimated in a straight-forward way using error propagation techniques (Taylor, 1982). All of the forward rate constants calculated from the LCM, with the exception of the filtration experiment conducted with 100 mM NaCl, fall within 1 standard deviation of the corresponding values of k_f calculated by the DBFM. The non-dispersive portion of the BTC corresponding to 100 mM NaCl exhibits a positive slope (see Fig. 1), which probably accounts for the differences in the forward rate constants calculated from the two models in this case.

The BTC obtained for a particular filtration experiment depends on the details of the experimental setup (e.g., column length, pore water velocity, etc.) and on the interaction forces that develop between virus and collector upon close approach. Significant insight into the latter phenomena can be obtained by calculating the filtration efficiency for each of the filtration experiments (see Materials and Methods). Physically, the filtration efficiency, α, represents the fraction of virus/collector collisions that result in a sticking event. As α approaches unity, every collision results in a sticking event and viruses are very effectively filtered by the quartz sand. As α decreases toward zero, an increasing number of viruses pass through the filter without being retained. Figure 2 presents calculated values of α

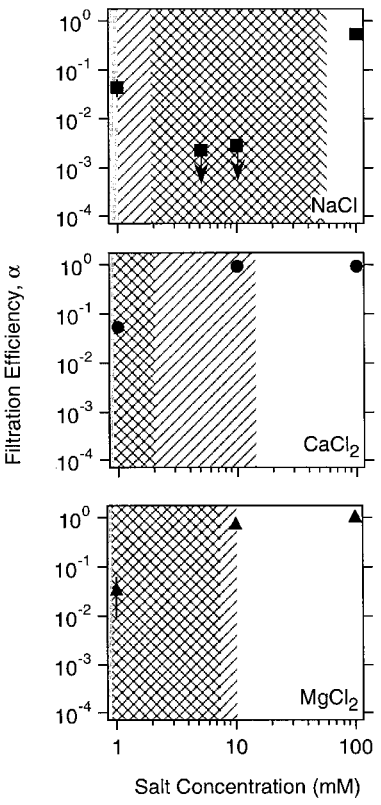

Fig. 2. Filtration efficiencies estimated from the breakthrough curves, plotted as a function of salt concentration. equation 1 and equation 6 were used to calculate filtration efficiencies. The arrows on the 5 and 10 mM NaCl data indicate they represent upper bounds. Error bars represent one standard deviation. The hatched regions represent ranges of cations present in rainwater (shaded region, Berner and Berner, 1987), groundwater (forward hatching, Faust and Osman, 1981) and wastewater (back hatching, Chang and Page, 1985).

plotted against salt concentration. These results are qualitatively consistent with the trends noted above for Fig. 1. Namely, filter performance increased with increasing salt concentration, and was improved if divalent cations were used in place of monovalent cations at the same concentration. An exception to this trend is the filtration efficiency calculated for 1 mM NaCl. For this condition $\alpha = 0.04$, which is much larger than the value of α estimated for either 5 or 10 mM NaCl ($\alpha < 3 \times 10^{-3}$). Possible reasons for the "anomalous" deposition of SJC3 in the presence of 1 mM NaCl will be discussed later in the paper.

Control experiments

Control experiments were performed to measure virus adsorption to the column apparatus for a subset of those experiments where appreciable virus filtration was observed –namely, 1 mM NaCl, 1 mM $MgCl_2$, and 100 mM $CaCl_2$. The control experiments were conducted in a manner similar to the filtration experiments, except that the columns contained no quartz sand. No adsorption to the column apparatus was observed for 1 mM NaCl and $MgCl_2$. Some column adsorption was observed in the presence of 100 mM $CaCl_2$ ($C/C_0 \approx 0.65$); however, this degree of adsorption is negligible compared to the 5 $\log_{10}$ reduction in virus concentration that occurred when the column was packed with quartz sand. In addition, bacteriophage inactivation in the stock 10 mM electrolyte solutions (NaCl, $CaCl_2$ and $MgCl_2$) was less than 1 $\log_{10}$ unit over a period of approximately 80 d (data not shown).

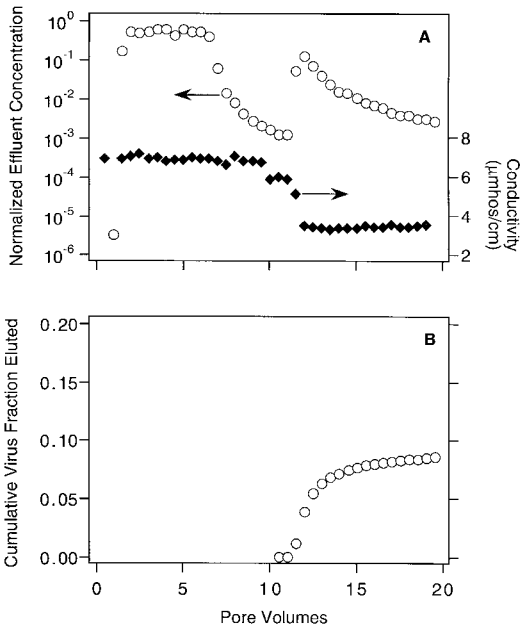

Fig. 3. (A) Normalized concentration of SJC3 in the column effluent for an elution experiment in which virus-containing 1 mM $CaCl_2$ solution was applied at the column influent for 5 pore volumes, followed by 5 pore volumes of virus-free 1 mM $CaCl_2$ and finally 10 pore volumes of virus-free 1 mM NaCl. The pulse of viruses eluted from the column beginning around pore volume 12 is coincident with the change in electrolyte composition of the effluent from 1 mM $CaCl_2$ to 1 mM NaCl, as indicated by the change in conductivity. (B) Cumulative fraction of previously adsorbed virus eluted by the 1 mM NaCl solution, calculated assuming no inactivation of previously deposited viruses.

Virus elution

To examine if changes in pore water chemistry might mobilize previously deposited bacteriophage, we conducted a single elution experiment with the following sequence of influent pulses: (i) approximately 5 pore volumes of a 1 mM $CaCl_2$ solution containing the bacteriophage isolate, (ii) 5 additional pore volumes of a bacteriophage-free 1 mM $CaCl_2$ solution, and (iii) 10 pore volumes of a bacteriophage-free 1 mM NaCl solution. The results of that experiment are presented in Fig. 3(A). The normalized effluent virus concentration initially increased to a steady-state value of $C/C_o \approx 0.53$, and then decreased as the virus-free $CaCl_2$ solution broke through at a pore volume of approximately 6. Importantly, when the virus-free 1 mM NaCl solution broke through around pore volume 12, it released a pulse of viruses that had been originally deposited in the column when the pore fluid consisted of 1 mM $CaCl_2$. Based on mass balance calculations and assuming that none of the deposited virus inactivated, we find that the pulse of virus released represented approximately 8 percent of the total viruses deposited during the initial phase of the experiment (see Fig. 3(B)). While other researchers have documented that changes in pore water conditions can lead to virus mobilization (Duboise *et al.*, 1976; Lance *et al.*, 1976; Landry *et al.*, 1979; Bales *et al.*, 1991), our results indicate that virus mobilization can occur in response to extremely small perturbations in the ionic strength of the system ($\Delta I = -2$ mM, where $I = \frac{1}{2}\sum_i c_i z_i^2$ and c_i and z_i are the concentration and valence of individual ions, i). It is also interesting to note that there was very little difference in the filtration efficiencies determined for 1 mM NaCl and 1 mM $CaCl_2$ (see Fig. 2). Hence, changes in the chemical composition of the pore fluid that do not appreciably influence the *forward* filtration of a virus, can still lead to the mobilization of previously deposited virus particles. The mechanism responsible for this elution event is likely to be complex for the ionic strength range employed here. In the presence of 1 mM NaCl, the filtration efficiency of the SJC3 virus is *inversely* correlated with salt concentration, which is counter to the trends observed in the presence of the divalent cations at 1 mM (compare the top and lower panels Fig. 2). Possible explanations for the anomalous deposition of the bacteriophage at 1 mM NaCl are presented in the section entitled Discussion.

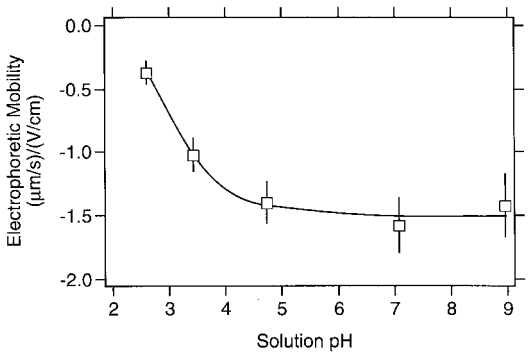

Fig. 4. Electrophoretic mobility of SJC3 in the presence of 10 mM NaCl and varying pH. Error bars represent one standard deviation.

Surface charge characterization

Filamentous bacteriophage such as SJC3 consist of a ssDNA molecule surrounded by a protein coat. Both the amino acid residues on the capsid and nucleotide linkages in the DNA backbone can ionize in solution, giving rise to a net surface charge on the virus that is pH dependent. The method of choice for characterizing the surface electrical potential of spherical colloidal particles is whole-particle microelectrophoresis, in which the velocity of individual particles (or electrophoretic mobility) is measured in the presence of an applied electric field. Electrophoresis measurements for non-spherical particles, such as SJC3, however, may not be so simply interpreted, as we discuss later. Figure 4 shows the results of microelectrophoresis measurements carried out on SJC3 in the presence of 10 mM NaCl and varying pH conditions. As might be expected, the electrophoretic mobility of the virus becomes more negative as the pH of the solution is increased, reflecting the deprotonation of ionizable amino acid and/or nucleic acid residues. Importantly, the bacteriophage appears negatively charged for all pH conditions tested in this study, ranging from pH 2.5 to 9. The pH at which the isolate has no electrophoretic mobility occurs below pH 2.5. Above pH 6, the electrophoretic mobility of SJC3 is relatively constant.

To assess if the electrostatic properties of SJC3 influence its filtration dynamics in the quartz sand filters, we measured the electrophoretic mobility of the virus at pH 7 and for the same set of electrolyte conditions employed in the filtration experiments (Fig. 5). In all cases, the absolute magnitude of the electrophoretic mobility decreased as the salt concentration increased. Charge reversal, the phenomenon whereby a negatively charged colloid becomes positively charged due to specific adsorption of a divalent cation, was not observed. For the three salts investigated in this study, the absolute mobility of the bacteriophage decreased approximately 60% when the salt concentration was increased from 1 to 100 mM. Also, the mobility of SJC3 in the presence of Ca^{2+} or Mg^{2+} is roughly one-half the observed mobility in the presence of Na^{+} at the same concentration. Within experimental error, the mobility of SJC3 is the same in the presence of either Ca^{2+} or Mg^{2+}. Hence, with respect to divalent cations, the mobility of this virus appears to depend only on the cation concentration, and not the specific cation employed.

DISCUSSION

The retention of SJC3 in our quartz sand filters was strongly influenced by the electrolyte composition of the pore fluid. With exception of the anomalous deposition observed at 1 mM NaCl, we found that SJC3 was better filtered when the ionic strength of the pore fluid was increased, either by (i) increasing the concentration of a particular salt or (ii) holding the salt concentration constant, but replacing the dominant cation with one of higher valence. Similar trends have previously been observed by other investigators employing soil columns and different viruses (Sobsey *et al.*, 1980; Taylor *et al.*, 1981; Lance and Gerba, 1984). At the solution pH employed in the filtration experiments presented here (pH 7), the surface of the quartz sand is negatively charged, and hence virus filtration occurs against an electrostatic barrier.

In general, the ability of a filter to remove charged colloidal particles from the fluid phase depends on the microscale interaction forces that develop as the particles approach the surface of individual grains in the filter, or "collectors". If the particles and collectors possess a like charge (as is the case for the filamentous bacteriophage/quartz sand system analyzed here), then the relevant interaction forces consist of electrostatic repulsive forces, attractive van der Waals forces, and possibly other repulsive forces including steric and hydration forces (Ryan and Elimelech, 1996). For spherical colloidal particles it is possible to calculate the electrostatic and van der Waals forces acting between a

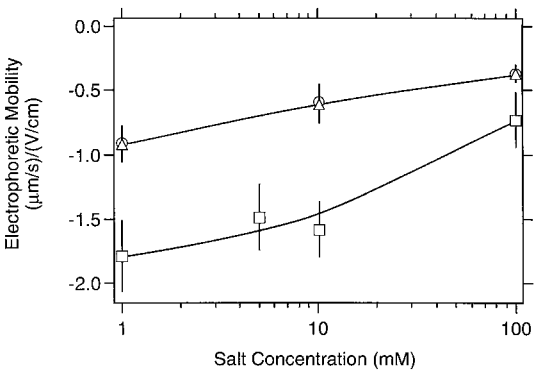

Fig. 5. Electrophoretic mobility of SJC3 as a function of salt concentration at pH 7. Error bars represent one standard deviation.

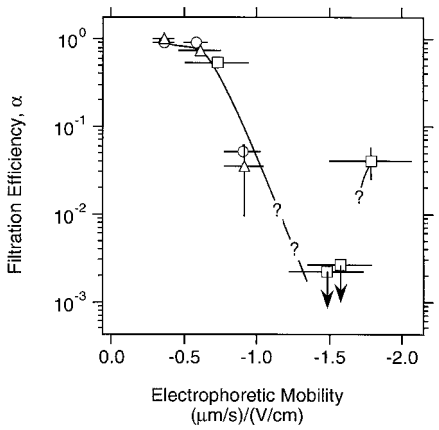

Fig. 6. Filtration efficiency of SJC3 plotted against the electrophoretic mobility of the virus in the presence of NaCl (squares), $CaCl_2$ (circles) and $MgCl_2$ (triangles). Arrows indicate upper bounds. Error bars represent one standard deviation.

particle and a collector as a function of separation distance using classic Derjaguin–Landau–Verwey–Overbeek (DLVO) theory (Derjaguin and Landau, 1941; Verwey and Overbeek, 1948). DLVO theory cannot be directly applied to our system because of the relatively complex geometry of filamentous bacteriophage, although the influence of electrostatic interactions on the filtration of SJC3 can still be assessed by comparing the filtration efficiency with the electrophoretic mobility of the virus measured under comparable solution conditions. This comparison, illustrated in Fig. 6, reveals that there is a general anticorrelation between the performance of the filter (as measured by the filtration efficiency) and the electronegativity of the virus (as measured by the electrophoretic mobility), in qualitative agreement with DLVO predictions. Our interpretation of this trend is that an increase in the ionic strength of the pore fluid screens the surface charge on the virus and collector, diminishes the electrostatic barrier to particle deposition, and consequently improves the overall performance of the filter, as illustrated schematically in Fig. 7(A). The exception to this rule is 1 mM NaCl, where appreciable virus filtration occurs despite the fact that SJC3 exhibits a very negative electrophoretic mobility.

One possible explanation for the anomalous deposition at 1 mM NaCl centers around the influence of solution ionic strength on the stiffness of filamentous bacteriophage. It is well known that single- and double-stranded DNA molecules in solution undergo a conformational transition from a rod-like state at 1 mM NaCl to a more flexible conformation at >5 mM NaCl (Hagerman, 1988). The class of filamentous bacteriophage analyzed here consists of a looped single-stranded DNA molecule that is packaged inside a protein coat so that two non-complementary strands of the DNA molecule run parallel to the long axis of the virus (Model and Russel, 1988). If DNA molecules packaged inside the protein coat behave similar to naked DNA in solution, then the filamentous bacteriophage may become more rod-like as the ionic strength is decreased to 1 mM NaCl. As illustrated in Fig. 7(B), this "stiffening" of the bacteriophage could lead to a change in the dominant deposition mechanism for the virus in the column, from

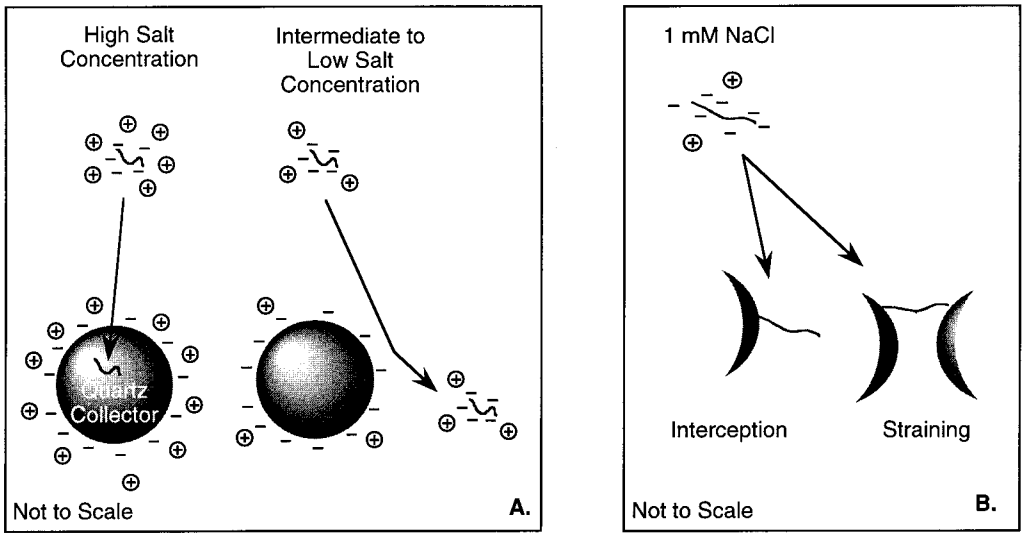

Fig. 7. Schematic diagram illustrating how electrostatic interaction forces may influence the filtration of SJC3 in quartz sand. (A) At low salt concentrations, electrostatic repulsive forces between the virus and the quartz grain inhibit filtration resulting in low filtration efficiency. As the salt concentration is increased, the negative surface charges are screened and the filtration efficiency is increased. (B) At 1 mM NaCl, SJC3 may exhibit a more rigid conformation, with non-Brownian mechanisms such as straining or interception dominating filtration dynamics.

Brownian diffusion at higher salt concentrations to interception and/or straining at lower salt concentrations. Alternatively, the virus/collector interaction forces may be more favorable at very low salt concentrations, as has been proposed for other systems (Elimelech, personal communication).

One of the more surprising outcomes of this study is that the apparent isoelectric point of SJC3 is less than 2.5, considerably lower than published values for other filamentous and non-filamentous viruses (Hobom and Braunitzer, 1967; Penrod *et al*., 1995, 1996; Redman *et al*., 1997). Whether or not an electrophoretic mobility value of zero at pH 2.5 corresponds to the true isoelectric point of the particle is likely to depend on its surface charge uniformity. Solomentsev and Anderson (1994) have modeled the electrophoretic motion of slender, rigid particles. Their models indicate that heterogeneously charged particles can move in an electric field even though the particle is neutral (zero-averaged zeta potential). For long slender cylinders, the more hydrodynamically exposed ends also exert a disproportionate influence on the particle's electrophoretic velocity. Unlike the particles modeled by Solomentsev and Anderson, filamentous bacteriophage are not entirely rigid and moreover, their conformation in likely to be a function of the electrolyte composition. Their surface charge characteristics are expected, however, to be relatively uniform based on their structure. Typically, filamentous bacteriophage are constructed from a total of five different proteins: multiple copies of a single protein (gene product VIII) that encapsulate the ssDNA core and cover the entire 900 nm length of the filament, and copies of four additional proteins (gene products III, VI, VII and IX) at both ends of the virus (Model and Russel, 1988). It is likely, therefore, that the charge characteristics of the main protein (gene product VIII) govern the electrophoretic behavior of the virus.

From an environmental perspective, these electrophoresis results suggest that SJC3 will be negatively charged over all pH conditions likely to prevail in natural groundwater systems. Given that bulk soil also tends to possess a net negative surface charge (Sposito, 1989) and using the present model system as a guide, we can postulate that the subsurface mobility of the filamentous bacteriophage is likely to be quite sensitive to the electrolyte composition of the pore fluid. For example, the elution experiment described earlier demonstrates that a change in the pore fluid electrolyte composition from 1 mM $CaCl_2$ to 1 mM NaCl –corresponding to a change in water hardness from 100 mg/l as $CaCO_3$ to approximately 0 mg/l– is sufficient to mobilize previously filtered SJC3 in the quartz sand columns. Variations in pore water hardness are observed in natural groundwater under the influence of recharge operations employing recycled wastewater and for groundwater under the influence of rainfall infiltration (see shaded regions in Fig. 2). Our results, therefore, suggest that filamentous bacteriophage trapped in the near-surface soil or sediment may be mobilized downward into groundwater following a modest decrease in the levels of hardness or TDS in the pore fluid. This conclusion is consistent with previous suggestions that filamentous bacteriophage and other viruses are mobilized in groundwater systems following prolonged rainfall (Wellings *et al*., 1975; Yanko *et al*., 1997). In addition, previous work involving poliovirus elution from soil columns has demonstrated that low TDS waters –such as distilled or artificial rainwater– are more likely to elute previously filtered virus than high TDS waters –such as wastewater (Duboise *et al*., 1976; Lance *et al*., 1976; Landry *et al*., 1979).

CONCLUSIONS

In this work we investigated the influence of pore water chemistry on the filtration and mobilization of a male-specific filamentous bacteriophage isolated from highly treated wastewater. Because of their male-specific nature and resistance to chlorination, this class of bacteriophage may be a useful indicator for potential fecal contamination in groundwater systems. We found that SJC3 has an apparent isoelectric point of less than pH 2.5 and that its electrophoretic mobility is roughly constant above pH 6. From a practical point of view, this implies that the surface electrical potential of this virus will not be significantly affected by the natural variability in pore water pH expected for most groundwater systems. On the other hand, we found that the filtration and electrostatic properties of SJC3 were dramatically influenced by the electrolyte composition of the pore fluid when the pH was held constant at 7. The filtration efficiency of SJC3 in quartz sand decreased with increasing salt concentration, in a manner consistent with DLVO theory. We found a strong anticorrelation between estimates of the filtration efficiency and the electrophoretic mobility of the virus, suggesting that virus deposition onto the quartz collector is inhibited by an electrostatic barrier. These results indicate that the electrolyte composition of the pore fluid, as reflected by TDS and hardness levels, may dramatically influence the filtration and mobilization of filamentous viruses in subsurface systems.

Acknowledgements—This work was sponsored by the NSF/EPA partnership for Environmental Research, under contract number DEB95-24481.

REFERENCES

Ackermann H. W. (1996) Frequency of morphological phage descriptions in 1995. *Arch. Virol*. **141,** 209–218.

Adams M. H. (1959) *Bacteriophages*, pp. 450–454. Interscience, New York, N.Y.

Bales R. C., Hinkle S. R., Kroeger T. W., Stocking K. and Gerba C. P. (1991) Bacteriophage adsorption during transport through porous media: chemical perturbations and reversibility. *Environ. Sci. Technol.* **25,** 2088–2095.

Berner E. K. and Berner R. A. (1987) *The Global Water Cycle*, p. 72. Prentice-Hall, Englewood Cliffs, N.J.

Chang A. C. and Page A. L., Soil deposition of trace metals during groundwater recharge using surface spreading. In *Artificial Recharge of Groundwater*, ed. T. Asano, p. 610. Butterworth, Boston, MA.

Dai H., Chiang K.-S. and Kuo T.-T. (1990) Characterization of a new filamentous phage Cf from *Xanthomonas citri*. *J. Gen. Virol.* **46,** 277–289.

Derjaguin B. V. and Landau L. (1941) Theory of the stability of strongly charged lyophobic sols and of the adhesion of strongly charged particles in solutions of electrolytes. *Acta Physicochim. U.S.S.R.* **14,** 300.

Duboise S. M., Moore B. E. and Sagik B. P. (1976) Poliovirus survival and movement in a sandy forest soil. *Appl. Environ. Microbiol.* **31,** 536–543.

Faust S. D. and Osman M. A. (1981) *Chemistry of Natural Waters*, pp. 1–58. Ann Arbor Science, Ann Arbor, MI.

Folk R. L. (1980) *Petrology of Sedimentary Rocks*, pp. 29–61. Hemphill Publishing Company, Austin, TX.

Grant S. B., List E. J. and Lidstrom M. E. (1993) Kinetic analysis of virus adsorption and inactivation in batch experiments. *Water Res.* **29,** 2067–2085.

Hagerman P. J. (1988) Flexibility of DNA. *Ann. Rev. Biophys. Biophys. Chem.* **17,** 265–286.

Havelaar A. H. and Pot-Hogeboom W. M. (1988) F-specific RNA-bacteriophages as model viruses in water hygiene: ecological aspects. *Water Sci. Technol.* **20,** 399–407.

Havelaar A. H., Vanolphen M. V. and Drost Y. C. (1993) F-specific RNA bacteriophages are adequate model organisms for enteric viruses in fresh water. *Appl. Environ. Microbiol.* **59,** 2956–2962.

Hedberg C. W. and Osterholm M. T. (1993) Outbreaks of food-borne and waterborne viral gastroenteritis. *Clin. Microbiol. Rev.* **6,** 199–210.

Hobom G. and Braunitzer G. (1967) Virusproteine, II. Untersuchung polycyclisher aromatisher Amine auf ihre mutagene Wirkung am phaged fd. *Hoppe-Seylers Z. Physiol. Chem.* **348,** 804–807.

IAWPRC Study Group on Health Related Water Microbiology *(1991) Bacteriophages as model viruses in water quality control. Water Res.* **25,** 529–545.

Johnson P. R. and Elimelech M. (1995) Dynamics of colloid deposition in porous media: blocking based on random sequential adsorption. *Langmuir* **11,** 801–812.

Keswick B. H. and Gerba C. P. (1980) Viruses in groundwater. *Environ. Sci. Technol.* **14,** 1290–1297.

Lance J. C. and Gerba C. P. (1984) Effect of ionic composition of suspending solution on virus adsorption by a soil column. *Appl. Environ. Microbiol.* **47,** 484–488.

Lance J. C., Gerba C. P. and Melnick J. L. (1976) Virus movement in soil columns flooded with secondary sewage effluent. *Appl. Environ. Microbiol.* **32,** 520–526.

Landry E. F., Vaughn J. M., Thomas McH. Z. and Beckwith C. A. (1979) Adsorption of enteroviruses to soil cores and their subsequent elution by artificial rainwater. *Appl. Environ. Microbiol.* **38,** 680–687.

Lawson H. W., Braun M. M., Glass R. I. M., Stine S. E., Monroe S. S., Atrash H. K., Lee L. E. and Englender S. J. (1991) Waterborne outbreak of Norwalk virus gastroenteritis at a southwest United-States resort: role of geological formations in contamination of well water. *Lancet* **337,** 1200–1204.

Litton G. M. and Olson T. M. (1993) Colloid deposition rates on silica bed media and artifacts related to collector surface preparation methods. *Environ. Sci. Technol.* **27,** 185–193.

Model P. and Russel M. (1988) Filamentous bacteriophage. In *The Bacteriophages*, ed. R. Calendar, Vol. 2, pp. 375–456. Plenum, New York, N.Y.

Penrod S. L., Olson T. M. and Grant S. B. (1995) Whole particle microelectrophoresis for small viruses. *J. Colloid Interface Sci.* **173,** 521–523.

Penrod S. L., Olson T. M. and Grant S. B. (1996) Deposition kinetics of two viruses in packed beds of quartz granular media. *Langmuir* **12,** 5576–5587.

Press W. H., Flannery B. P., Teukolsky S. A. and Vetterling W. T. (1986). *Numerical Recipes*. Cambridge University Press, New York, N.Y.

Rajagopalan R. and Chu R. Q. (1982) Dynamics of adsorption of colloidal particles in packed beds. *J. Colloid Interface Sci.* **86,** 299–317.

Reddy K. R., Khaleel R. and Overcash M. R. (1981) Behavior and transport of microbial pathogens and indicator organisms in soils treated with organic wastes. *J. Environ. Qual.* **10,** 255–266.

Redman J. A., Grant S. B., Olson T. M., Hardy M. E. and Estes M. K. (1997) The filtration of recombinant Norwalk virus particles and bacteriophage MS2 in quartz sand: importance of electrostatic interactions. *Environ. Sci. Technol.*, in press.

Ryan J. N. and Elimelech M. (1996) Colloid mobilization and transport in groundwater. *Colloids and Surfaces A* **107,** 1–56.

Snowdon J. A. and Cliver D. O. (1989) Coliphages as indicators of human enteric viruses in groundwater. *Crit. Rev. Environ. Control* **19,** 231–249.

Sobsey M. D., Dean C. H., Knuckles M. E. and Wagner R. A. (1980) Interactions and survival of enteric viruses in soil materials. *Appl. Envion. Microbiol.* **40,** 92–101.

Solomentsev Y. and Anderson J. L. (1994) Electrophoresis of slender particles. *J. Fluid Mech.* **279,** 197–215.

Sposito G. (1989) *The Chemistry of Soils*, pp. 127–147. Oxford University Press, New York, N.Y.

Taylor D. H., Moore R. S. and Sturman L. S. (1981) Influence of pH and electrolyte composition on adsorption of poliovirus by soils and minerals. *Appl. Environ. Microbiol.* **42,** 976–984.

Taylor J. R. (1982) *An Introduction to Error Analysis*, pp. 40–80. University Science Books, Mill Valley, CA.

Verwey E. J. W. and Overbeek J. Th. G. (1948) *Theory of the Stability of Lyophobic Colloids*. Elsevier, New York, N.Y.

Waldor M. K. and Mekalanos J. J. (1996) Lysogenic conversion by a filamentous phage encoding cholera toxin. *Science* **272,** 1910–1914.

Wellings F. M., Lewis A. L., Mountain C. W. and Pierce L. V. (1975) Demonstration of virus in groundwater after effluent discharge onto soil. *Appl. Microbiol.* **29,** 751–757.

Woody M. A. and Cliver D. O. (1995) Effects of temperature and host cell growth phase on replication of F-specific RNA coliphage QB. *Appl. Environ. Microbiol.* **61,** 1520–1526.

Yanko W. A., Jackson J. L., Williams F. P., Walker A. S. and Castillo M. S. (1998) An unexpected temporal pattern of coliphage isolation in groundwaters sampled from wells at varied distances from reclaimed water recharge sites. *Water Res.*

Yao K.-M., Habibian M. T. and O'Melia C. R. (1971) Water and waste water filtration: concepts and applications. *Environ. Sci. Technol.* **5,** 1105–1112.